water

MDPI

Article

Morphodynamic Controls on Thermal Plume Dispersion at River Mouths: Insights from Field Data and Numerical Modeling

Naghmeh Heidari [1], Murat Aksel [2], Oral Yagci [3], Mehmet Yusuf Erbisim [4], Sevket Cokgor [1] and Manousos Valyrakis [5,*]

[1] Division of Hydraulics, Civil Engineering Department, Istanbul Technical University, Istanbul 34469, Türkiye; naghmeh88heidari@gmail.com (N.H.); cokgor@itu.edu.tr (S.C.)
[2] Civil Engineering Department, Alanya Alaaddin Keykubat University, Alanya 07425, Türkiye; murat.aksel@alanya.edu.tr
[3] Civil Engineering Department, Engineering Faculty, Aydin Adnan Menderes University, Aydin 09010, Türkiye; oral.yagci@adu.edu.tr
[4] HEC Engineering Co., Istanbul 51000, Türkiye; mehmet@hec-engineering.com
[5] Faculty of Civil Engineering, Aristotle University of Thessaloniki, 54124 Thessaloniki, Greece
* Correspondence: mvalyra@civil.auth.gr

Abstract

Thermal discharge from power plants causes significant concerns in aquatic environments. The purpose of this study is to evaluate how river mouth morphodynamics, particularly spit development and removal, influence the dispersion of thermal plumes. To achieve this, a case study was carried out at a coastal power plant in southwest Türkiye, where thermal effluent is conveyed to the sea through a low-flow river. Field measurements combined with numerical modeling were used to analyze plume dynamics under varying spit configurations. Results revealed that the evolution of a spit on one side of the river mouth influences plume dispersion and redirects the mixing zone toward the opposite shoreline. Numerical simulations demonstrated that spit development reduces dispersion efficiency (by over 75%), while the physical removal of the spit significantly improves it, reducing temperature excess from 4–5 °C to 0–1 °C within the mixing zone, meeting safe environmental standards. The findings highlight the pivotal role of morphological changes in governing thermal discharge behavior and emphasize the importance of continuous monitoring and management strategies, such as periodic dredging, to ensure compliance with environmental regulations.

Keywords: thermal discharge; river mouth morphodynamics; thermal plume; mixing zone; spit development

Academic Editor: Bommanna Krishnappan

Received: 11 August 2025
Revised: 8 September 2025
Accepted: 11 September 2025
Published: 14 September 2025

Citation: Heidari, N.; Aksel, M.; Yagci, O.; Erbisim, M.Y.; Cokgor, S.; Valyrakis, M. Morphodynamic Controls on Thermal Plume Dispersion at River Mouths: Insights from Field Data and Numerical Modeling. *Water* **2025**, *17*, 2721. https://doi.org/10.3390/w17182721

1. Introduction

Thermal discharge from power plants into water bodies has detrimental effects on water quality and aquatic life. Concerns with the dispersion of thermal pollution have led to investigation of heated water behavior in greater detail. Thermal pollution refers to any change in environmental temperature caused by industrial cooling processes [1]. The cooling system of a power plant is designed to dissipate excess heat during thermal transients, electricity generation, and auxiliary processes to prevent overheating and maintain efficiency [2]. One of the main types of cooling systems is known as a "once-through cooling system" [3]. Once-through cooling systems in both thermal [4,5] and nuclear power plants [6] use water from natural resources and discharge it back into the source after

circulating in the system and absorbing the excess heat. Although due to the high heat capacity of a water body, its mean temperature may not be significantly influenced by thermal discharges, localized temperature rises can disrupt the ecological balance of the region [7]. Therefore, industrial cooling effluent is considered a threat to coastal areas.

A thermal plume, which refers to water that is remarkably warmer than the ambient water, rises and spreads at the sea surface due to its lower density. Trajectory, mixing, and retention are the main components of the thermal dispersion. Regulations governing industrial thermal plumes vary by climate zone. Continuous monitoring and evaluation of sea temperature data in areas affected by thermal discharges are essential to ensure compliance with these standards. According to Bleninger and Jirka [8], regulations in European climate regions specify that the temperature increase caused by thermal effluents should not exceed +3 °C above the ambient water temperature at the edge of the mixing zone (typically a distance of 100 m from the shoreline). A mixing zone is defined as a region near the discharge point where effluent is initially diluted and water quality criteria can be temporarily exceeded [9]. It is worth mentioning that both the discharge location of the thermal effluent [10] and the meteorological conditions [11] determine the trajectory and mixing mechanism of the plume. On the other hand, the plume residence time is predominantly governed by discharge conditions [12].

The extent and direction of the thermal plume spread depend mainly on the wind speed, sea currents, and tidal condition [13,14]. However, not all thermal plumes are directly discharged into the sea, as some are transported by rivers. Existing river characteristics play a prominent role during the initial dispersion process of the thermal effluent. Numerous factors can be mentioned among the influential features in the riverine domain, e.g., river corridor morphology, location of thermal discharge, ambient temperature of the river, temporal variation of flow pattern, sediment concentration, climate condition, and river–sea interactions. Additionally, when a river is the source of thermal discharge, morphology of the river mouth emerges as a pivotal factor. Incorporating all aforementioned river characteristics in the evaluations is a very sophisticated task. Hence, the factors with the pronounced impact are typically prioritized.

Researchers can explore thermal plumes through field surveys, remote sensing, numerical modeling, or combinations of these methods. However, no single method typically suffices to provide comprehensive results on its own. In the past, researchers have conducted various studies to examine the characteristics of thermal discharge and its environmental consequences. One of the numerical tools that has high capability in integrating wave, sediment, and bathymetric conditions in modeling of the thermal plume dispersion is Delft3D software. Although dispersion of thermal discharge in the sea [15–17] or estuaries [18] has been analyzed using Delft3D in the pertinent literature, the influence of river mouth morphodynamics has not been addressed to date. While earlier studies have examined thermal plume dispersion in estuarine or coastal waters, none have systematically evaluated the influence of evolving river mouth morphology—especially spit growth and removal—on compliance with thermal discharge regulations. In this research, the authors focused on the spit development process in the river mouth and its impact on thermal plume dispersion. Unlike previous investigations that considered plume dispersion in static environments, this study explicitly quantifies the role of dynamic spit morphodynamics in altering thermal mixing behavior.

River mouth spits are depositional features extending from one end of the mainland into the sea [19], typically found in wave-dominated deltas [20]. These landforms develop through self-organizing processes driven by shoreline instability, which leads to asymmetrical topography of the river mouth [21]. The influential role of topography in the direction of thermal plume dispersion was demonstrated by Cheng and Hao [22] using a

3D numerical model based on k-ε turbulence closure. However, the unstable geomorphic units (e.g., spits) introduce additional complexity into such evaluations. Consequently, further investigation is required to account for the impact of these landforms. Dan et al. [23] stated that when the sediment supply surpasses the capacity of wave-driven transport, it triggers the formation and evolution of the river mouth spit. The orientation and length of the spits are changeable [24] because of wave direction [25], wind condition [26], and seasonal cycles [27]. As a result, thermal dispersion behavior can be significantly altered due to complex interactions between the plume and variable morphological setting induced by spit development.

The present study examines the impact of river mouth morphodynamics on thermal plume dispersion of a power plant in the southwest of Türkiye. The primary objective of this study is to evaluate how river mouth morphodynamics, particularly spit development and removal, influence the dispersion of thermal plumes from a coastal power plant in southwest Türkiye, and to determine whether the resulting thermal discharge complies with water quality regulations. Understanding this issue is crucial for designing effective monitoring and management strategies to minimize environmental impacts. Since the plume behavior was directly influenced by river mouth morphology, the assessments were focused on the spit development/removal processes. For this purpose, (a) the spit evolution patterns and shoreline dynamics were extracted from satellite imagery, (b) oceanographic data were continuously collected in the field through the buoy system, and (c) numerical modeling was implemented to evaluate the role of spit on the hydrodynamics of the thermal dispersion process.

2. Methodology

2.1. Case Study

We studied a coal-fired thermal power plant located in the southwest of Türkiye (Figure 1) that plays an important role in the country's energy landscape, with an installed capacity of 630 MW and annual electricity generation of approximately 4.1 TWh per year. The once-through cooling system of the power plant draws the cooling water from Gökova Gulf. The water intake is supplied from a depth of −10 m below the sea surface elevation via a 2.5 m wide channel. Unlike the water intake, which is drawn directly from the gulf, the thermal effluent travels from the cooling facility to the system outlet in the river. Subsequently, the river conveys the cooling water discharge to the gulf. The overall transfer distance is about 2 km.

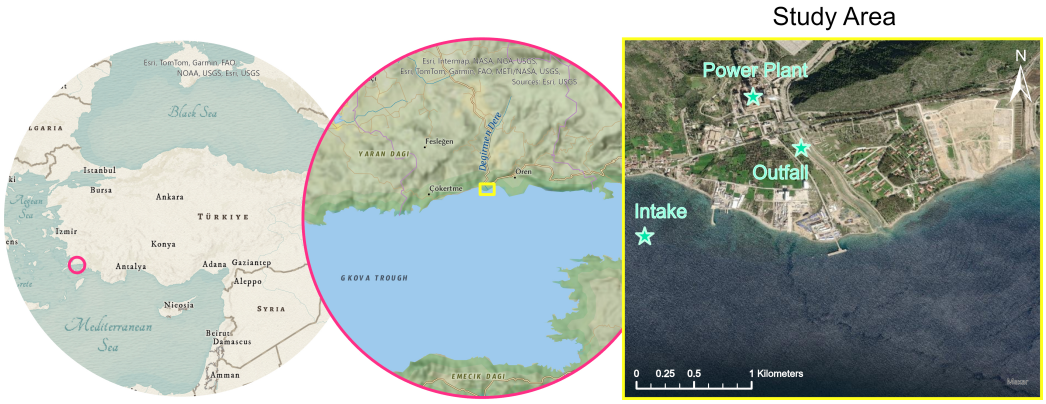

Figure 1. Location of the study area.

2.2. Field Measurements

Gökova Gulf is subject to strong and highly variable winds, which result in differences in current vectors between the surface water and the underlying water mass. The current

conditions along with the morphological setting and sediment characteristics of the estuary lead to spit development in the mouth of the river. It is important to note that the spit persistently migrates in the direction dominated by the coastal current.

The preference for the river as the discharge location, rather than the shoreline, was driven by accessibility and the river's favorable conditions for accommodating the thermal discharge. The studied river is characterized by very low-flow conditions. The river has been channelized with concrete, resulting in a highly controlled flow path. This condition allowed us to focus on the influence of spit development/removal on thermal effluent, since the minimal river discharge had no significant impact on it. The low-flow conditions reduce the complexity of the thermal discharge dispersion by confining the heat dissipation area and reducing the probability of abrupt changes in the dispersion process.

The study was conducted in the nearshore region, employing a network of buoys (Figure 2a). The monitoring systems were deployed at multiple locations that were strategically selected based on bathymetry. Bathymetric measurements were carried out over a sufficiently large area to encompass the region affected by thermal discharge. More importantly, efforts were made to ensure that the measured data would represent the area influenced by thermal discharge dispersion. Bathymetric data were collected using multibeam sonar to obtain high-resolution measurements of seafloor topography. Additional measurements were taken with a theodolite positioned onshore to accurately locate surface reference points.

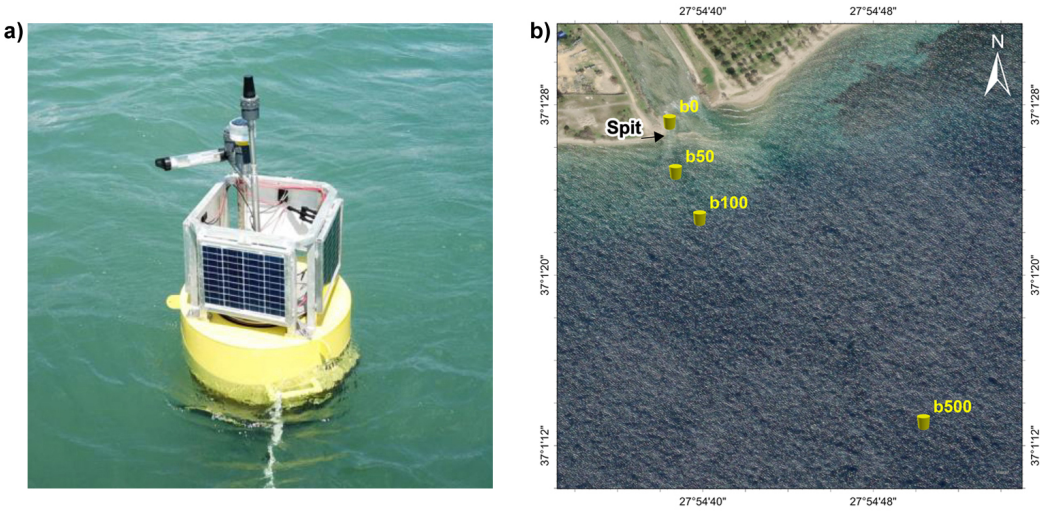

Figure 2. (**a**) View of a measuring system (i.e., oceanographic buoy) in the sea and (**b**) location of buoys in the study area.

For oceanographic measurements, the mooring buoy system was chosen. The mooring buoy, anchored to the seabed and connected via a mooring line, is designed for continuous, real-time monitoring of oceanographic parameters [28]. The buoys measured sea water temperatures at different distances from the coastline. The water depth at the measuring points and detailed information about buoy positions are presented in Table 1. The location of buoys was selected for their ability to reflect the oceanographic conditions of the region (Figure 2b). During 2020 and 2021, continuous data collection (including temperature measurements and periodic assessments of current velocity, density, and salinity) was carried out using monitoring systems to serve as the basis for the numerical model. The buoy was equipped with a surface-mounted data logger, GPS for positioning, and a thermistor-based temperature sensor. The accuracy of the mooring buoy system for surface water temperature was ±0.1 °C, with a resolution of 0.01 °C. The position of buoys was maintained within a radius of approximately 10–20 m from the deployment coordinates. The first buoy

(*b0*) was deployed at the river mouth, while the last buoy (*b500*) was designated as the reference case. The reference buoy was positioned at an appropriate distance from the thermal mixing zone, ensuring that it measures ambient water temperature, unaffected by localized thermal influences. Throughout the study, the positions of *b50* and *b100* were strategically altered to collect data from the affected area by thermal discharge.

Table 1. Spatial and installation information of the monitoring points.

Buoy	Planar Distance (m)	Depth (m)	Latitude (°N)	Longitude (°E)
b0	0	0.5	37.0242	27.9107
b50	50	2.5	37.0236	27.9108
b100	100	8.5	37.0230	27.9111
b500	500	39.5	37.0213	27.9152

To assess the influence of river mouth morphodynamics on the thermal dispersion, the spit evolution patterns were analyzed in detail. Temporal modifications of spit were examined using satellite imagery from Google Earth Pro, allowing visual comparison of spit morphology over time (Figure 3). At the end of May 2020, field activities were carried out to enhance dispersion efficiency through the physical removal of the spit. Consequently, evaluations were performed for both the presence and absence of spit. In Figure 3, (a) to (f) illustrate the morphological changes of the spit from 2004 to 2021, based on satellite imagery, and (g) presents an aerial photograph of the spit taken prior to the removal activities conducted in 2020.

Figure 3. Temporal evolution of spit: (**a**–**f**) satellite imagery and (**g**) aerial drone photograph.

2.3. Numerical Model

For accurate and reliable performance of monitoring systems, it is important to ensure that the buoys are negligibly affected by environmental variables. The primary challenges for buoy systems arise from the forces generated by waves and river discharge, which can disrupt buoy positioning. To better understand the impact of these forces, hydrodynamic modeling was implemented to analyze the coastal morphodynamics effect (i.e., spit development) on the process of thermal dispersion in the region.

Delft3D, a numerical modeling software, was utilized to simulate and analyze the interplay of wave, current, and coastal morphology changes using its various modules. The FLOW module, a key component of Delft3D, is a multidimensional hydrodynamic modeling program that can simulate flow and transport processes. For thermal dispersion analysis, the FLOW module was operated, while the wave characteristics at the buoy monitoring locations were applied to the WAVE module. Temperature and bathymetric data, along with the climate data acquired from the Turkish Coastal Wind and Wave Atlas, were incorporated into the model. In the WAVE module, 0.5 m, 1 m and 1.5 m waves were defined separately from the south and southwest directions, as detailed in Table 2.

Table 2. Wave characteristics selected for the scenarios.

Scenario	Direction	Height (m)	Period (s)
1	South	0.5	4
2	South	1.0	4
3	South	1.5	4
4	Southwest	0.5	4
5	Southwest	1.0	4
6	Southwest	1.5	4

To capture the variability in hydrodynamic conditions due to morphological configuration of the river mouth, the numerical model was run for multiple spit conditions. Five spit morphology scenarios, including configurations with no spit and spits extending 10, 20, 30, and 40 m, were incorporated into the model setup. These combinations of wave and morphological conditions allowed for a comprehensive analysis of their influence on thermal plume behavior and dispersion efficiency. These cases allowed for a systematic investigation of spit length on the behavior of thermal plumes and the hydrodynamic response of the system.

Delft3D-FLOW solves the unsteady, free-surface flow equations, and it integrates the Navier–Stokes equations with the heat transport equation to account for temperature variations. The Navier–Stokes equations governing the flow hydrodynamics are given below:

$$\frac{\partial u}{\partial t} + u\frac{\partial u}{\partial x} + v\frac{\partial u}{\partial y} + w\frac{\partial u}{\partial z} = -\frac{1}{\rho}\left(\frac{\partial p}{\partial x}\right) + \nu\left(\frac{\partial^2 u}{\partial x^2} + \frac{\partial^2 u}{\partial y^2} + \frac{\partial^2 u}{\partial z^2}\right) + f_x \quad (1)$$

$$\frac{\partial v}{\partial t} + u\frac{\partial v}{\partial x} + v\frac{\partial v}{\partial y} + w\frac{\partial v}{\partial z} = -\frac{1}{\rho}\left(\frac{\partial p}{\partial y}\right) + \nu\left(\frac{\partial^2 v}{\partial x^2} + \frac{\partial^2 v}{\partial y^2} + \frac{\partial^2 v}{\partial z^2}\right) + f_y \quad (2)$$

$$\frac{\partial w}{\partial t} + u\frac{\partial w}{\partial x} + v\frac{\partial w}{\partial y} + w\frac{\partial w}{\partial z} = -\frac{1}{\rho}\left(\frac{\partial p}{\partial z}\right) + \nu\left(\frac{\partial^2 w}{\partial x^2} + \frac{\partial^2 w}{\partial y^2} + \frac{\partial^2 w}{\partial z^2}\right) + f_z + G_z \quad (3)$$

where u and v are the horizontal velocities in the x and y directions, respectively; w is the vertical component of velocity; ρ is the fluid density; p is the pressure; f_x, f_y, and f_z are the viscous accelerations; and G_z is the gravitational acceleration.

As water temperature is influenced by thermal discharge, the heat transfer equation presented below should be solved:

$$\frac{\partial T}{\partial t} + u\frac{\partial T}{\partial x} + v\frac{\partial T}{\partial y} + w\frac{\partial T}{\partial z} = \frac{\partial}{\partial x}\left(\alpha\frac{\partial T}{\partial x}\right) + \frac{\partial}{\partial y}\left(\alpha\frac{\partial T}{\partial y}\right) + \frac{\partial}{\partial z}\left(\alpha\frac{\partial T}{\partial z}\right) + S_T \quad (4)$$

where T is the temperature field; α is the thermal diffusivity; S_T is the source term for thermal discharge.

2.4. Initial and Boundary Conditions

To simulate the behavior of the thermal plume, initial and boundary conditions were specified based on field measurements. A summary of these conditions used in the numerical modeling is given in Table 3. Additionally, an overview of the methodological steps followed in this study is presented in Figure 4.

Table 3. Initial and boundary conditions.

Parameter	Value
Water level	0 m
Ambient sea water temperature (summer condition)	27 °C
Discharge temperature	31 °C
Salinity	39 PSU
Domain features	High-resolution
Boundary condition (seabed)	No-slip wall

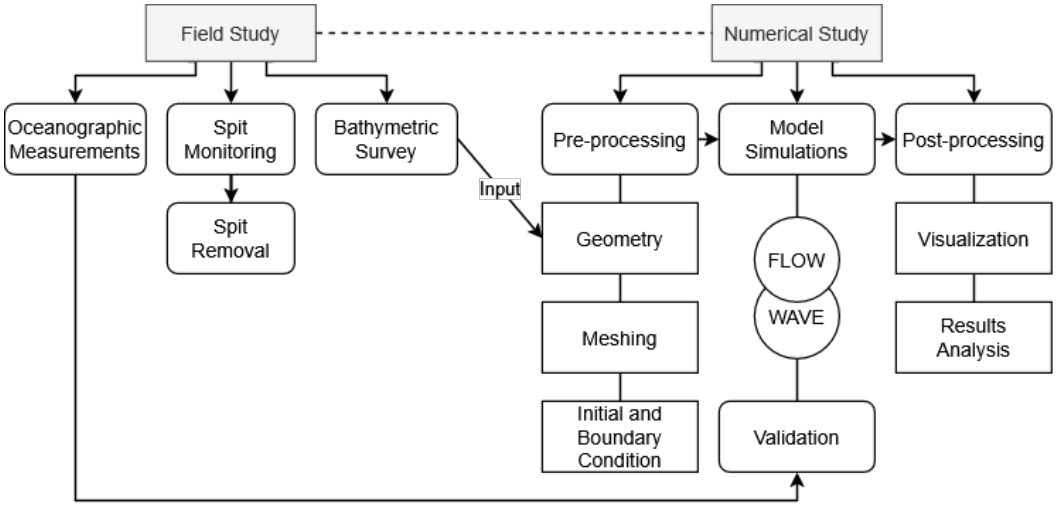

Figure 4. Flowchart of the methodology.

3. Results

3.1. Field Study Observations

3.1.1. Morphometry of River Mouth Spit

The aim of this section is to deal with the temporal changes in spit morphometry observed during the monitoring period. The formation of a river mouth spit reflects the combined influence of the prevailing river flow pattern, which controls the quantity of sediment delivered to the sea, and the littoral drift acting along the shoreline. In natural rivers, the helical flow developing within the channel cross-section plays a key role in determining sediment transport to coastal water [29].

To better conceptualize the morphometric values, the characteristic parameters defined for the river mouth spit are illustrated in Figure 5. As shown in the figure, these metrics are

the spit-generated bay length (L), the spit width (w), and the offset distance between the spitline and the bankline (s) which are parallel to each other. The temporal changes in these morphometric characteristics are obtained based on Figure 3 and summarized in Table 4, providing a quantitative view of the spit evolution.

The temporal evolution (Figure 5) indicates that the spit initially develops laterally toward the river centerline, thereby narrowing the active mouth area and consequently increasing the outlet velocity to the sea. This intensified flow pattern was particularly evident in March 2009 (Figure 3), when deepening of the active channel was also clearly observable. By April 2013, however, the spit head began to deflect inward toward the river channel. This morphological formation likely increased the hydraulic resistance to flow and intensified the helicity of the existing secondary circulation, thereby reinforcing helical flow structures within the channel. As previously detailed by [30,31], such enhancement of flow helicity associated with river mouth spits may also trigger the development of midchannel islands near the river mouth, further amplifying hydraulic resistance as can be verified from Figure 3.

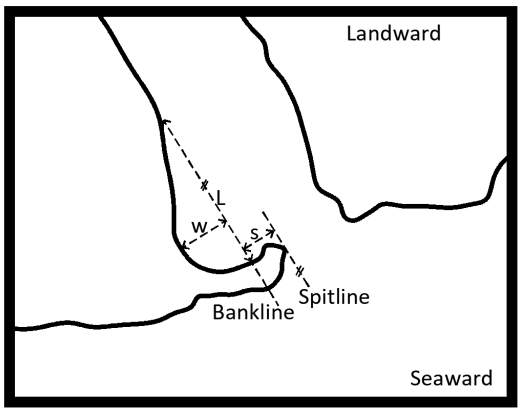

Figure 5. Conceptual figure which defines the morphometric variables examined during the morphometric analysis.

Table 4. Temporal change in morphometric characteristics of the river mouth spit.

	L (m)	w (m)	s (m)	$w + s$ (m)
June 2004	39.415	5.832	6.902	12.734
March 2009	88.158	17.924	4.703	22.627
April 2013	61.305	17.907	5.111	23.018
April 2016	75.768	6.902	9.883	16.785
November 2020	77.143	16.524	9.039	25.563
March 2021	65.758	17.049	N/A	17.049

3.1.2. Bathymetry

Figure 6 presents the bathymetry of the study area, highlighting temporal changes near the river mouth (a–c) and the longitudinal profile of the bottom slope (d). Figure 6a reveals that the bottom slope remains relatively constant alongshore, and the depth variation predominantly occurs in the cross-shore direction. Notably, the evolution of the spit at the river mouth is evident in the bathymetric maps from 2021 to 2023. Following the spit removal in 2020, a new spit began to form. Therefore, there are observable changes in the contour lines near the river mouth, reflecting ongoing spit growth. The cross-sectional profile in Figure 6d indicates that the slope has two segments, which can result from wave action and coastal erosion. The initial segment, extending up to 90 meters, exhibits a gradual and uniform slope (approximately 5%), while beyond this distance, the slope becomes steeper.

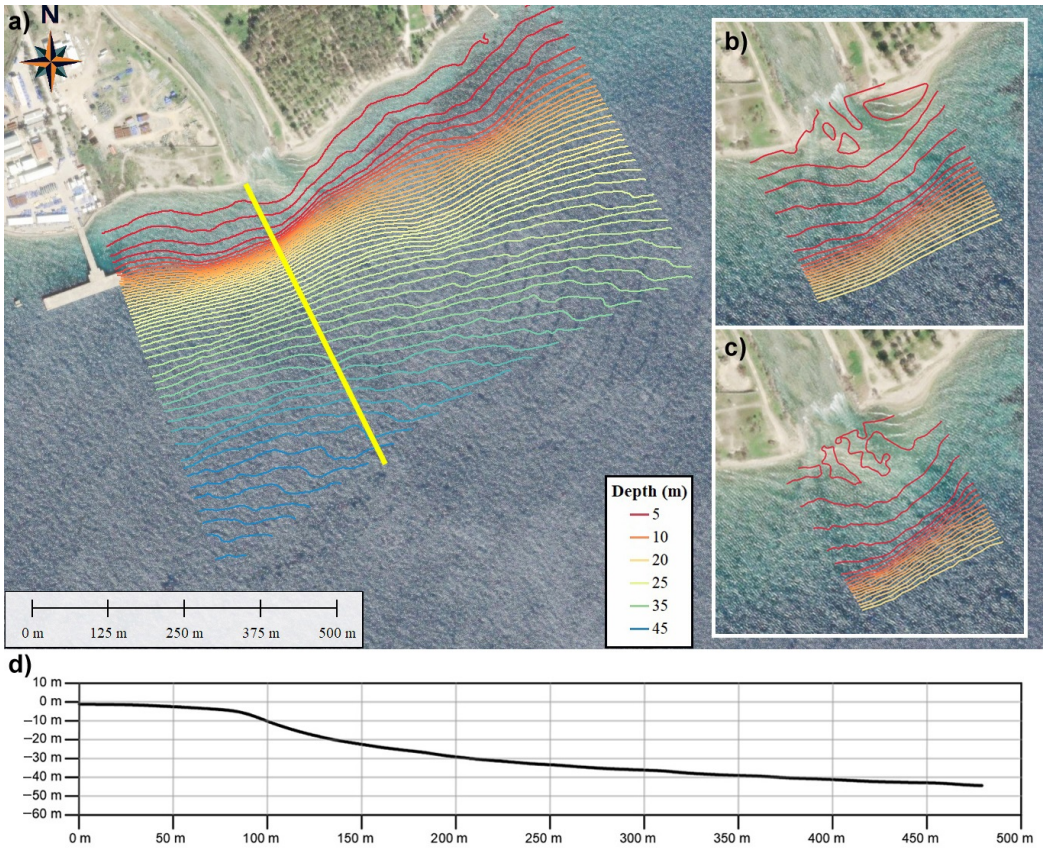

Figure 6. Bathymetric maps of the study area for (**a**) 2021, (**b**) 2022, and (**c**) 2023. (**d**) Longitudinal profile depicting the bottom slope along the yellow transect indicated in (**a**).

3.1.3. Oceanography

Sea surface temperature measurements collected from monitoring buoys were compared with reference values at 500 meters. In this analysis, erroneous or physically implausible readings were removed through appropriate filtering techniques. Monthly average temperature values were then calculated from the validated data. The temperature measured at *b500* was 27 °C. This value was subtracted from the temperatures at *b0*, *b50*, and *b100* to calculate the heat excess.

Figure 7 shows the monthly average temperature differences measured at various monitoring points relative to a reference point (i.e., *b500*), which is representative of the ambient water temperature. The data cover the period from January 2020 to August 2021. The lack of data in May 2020 is due to an intervention that took place that month to enhance thermal dispersion efficiency by removing the river mouth spit. This intervention is reflected in the temperature difference trends presented in Figure 7. Prior to the spit removal, the temperature difference between *b0* and *b500* fluctuated between 4 °C and 5 °C. Following the spit removal, a notable decrease in temperature differences was observed. This reduction is particularly evident when comparing the same months in the subsequent year.

In addition, the higher temperature differences from October to January are attributed to lower ambient water temperatures during these months, while the thermal discharge temperature does not vary markedly throughout the year. Since *b0* corresponds to the river mouth where the thermal plume is released and the discharged water is not yet diluted by the sea, the temperature difference (*b0–b500*) remains high in colder months. In contrast, *b50* and *b100* are located farther into the sea where plume dilution occurs. At these points, the influence of the colder ambient water suppresses the plume temperature, resulting in much smaller seasonal variations in the differences (*b50–b500*) and (*b100–b500*).

A similar reduction trend is also observed for the temperature differences between *b50* and *b500*, as well as *b100* and *b500*. After February 2021, when the ambient water temperature began to rise again, the temperature differences at all three monitoring points (i.e., *b0*, *b50*, and *b100*) fluctuate between 0 °C and 1 °C. This consistent reduction in temperature differences at monitoring points demonstrates the significant impact of the river mouth spit removal on improving the efficiency of thermal dispersion.

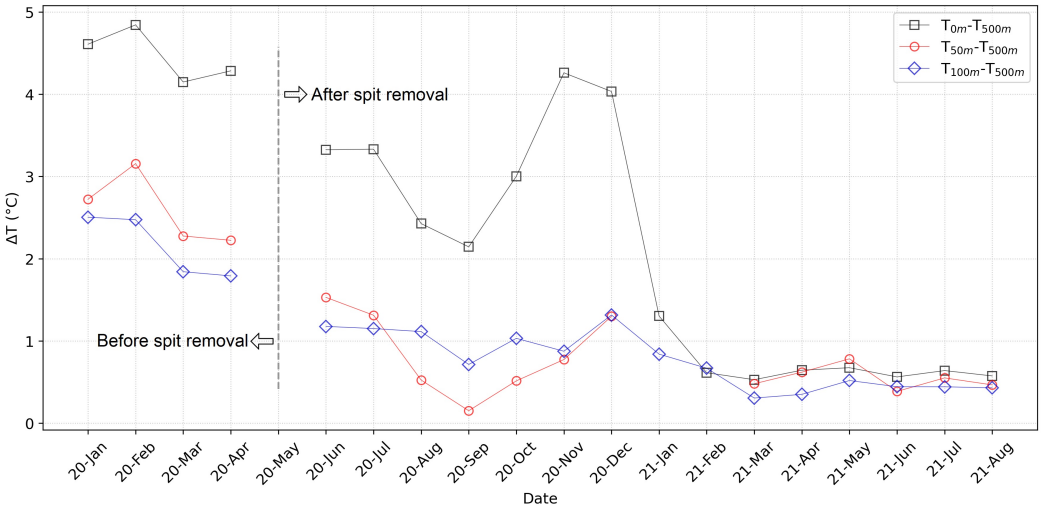

Figure 7. Monthly average temperature differences at monitoring points relative to the reference point; January 2020–August 2021.

As spit development is a dynamic process, the temperature differences were also calculated for the acquired data from March 2023 to February 2024. Figure 8 shows the monthly average temperature differences at monitoring points relative to the reference point during this period. It is evident that with the new spit development, clearly visible in the bathymetric maps (Figure 6), the temperature difference values have slightly increased. Nevertheless, these values remain lower than those recorded in 2020, indicating that the spit is still in its early stages of development.

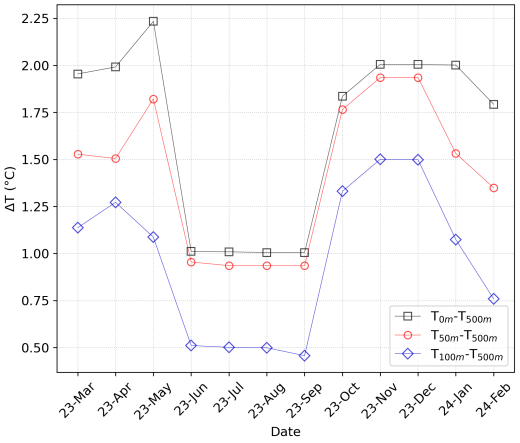

Figure 8. Monthly average temperature differences at monitoring points relative to the reference point; March 2023–February 2024.

3.2. Thermal Discharge Dispersion

Figure 9 represents the spatial distribution of water temperature in the area influenced by the thermal plume. Each subfigure corresponds to a different morphological configuration at the river mouth. The cross marks in the subfigures denote the locations of *b50*

and *b100*, which were adjusted during the field surveys to capture thermal data near the plume edge. Figure 9a depicts the dispersion pattern of thermal discharge following the spit removal. Figure 9b–e present scenarios reflecting different stages of spit evolution, with respective lengths of 10, 20, 30, and 40 m. These morphological configurations were derived from satellite observations.

In the absence of the spit, the thermal plume exhibits an almost symmetrical dispersion pattern, with the maximum temperatures observed along the river's centerline. The results of numerical modeling show that at the 100-m regulatory threshold distance, the temperature values range between 27.8 °C and 28.3 °C. As the spit elongates, the plume becomes increasingly asymmetrical, and the dispersion direction shifts toward the west coast, resulting in the extension of the thermal influence beyond the 100-m threshold.

The temperature differences between the ambient water (27 °C) and the plume edge in the numerical simulations align well with in situ oceanographic measurements. The removal of the spit significantly mitigates the thermal impact, limiting the temperature excess at the edge of the mixing zone to approximately 1.4 °C, as shown in Figures 7 and 9. The worst thermal condition is observed during the winter, when the ambient water temperature is lower than that of the thermal discharge.

Since the monitoring buoy positions were relocated progressively from left to right to track temperature variations, Figure 10 reveals a distinct pattern influenced by spit development. In the first and second buoy positions, the water temperature decreased as the spit extended, whereas in the third and fourth positions, the temperature increased. This spatial variation indicates that spit growth alters the dispersion of the thermal plume, redirecting its path and influencing local thermal conditions.

Calibration and Validation

Calibration of the numerical model was previously performed using available field measurements and historical hydrodynamic data. The current study did not involve additional calibration adjustments, and the model configuration was adopted as provided. After the spit removal activity, validation was carried out for summer conditions in 2021. During this period, monitoring buoys were relocated three times in July, August, and September, respectively. This allowed for spatially distinct observational datasets during the validation period.

A comparison between the observed monthly mean water temperatures and simulated values near the edge of the mixing zone is presented in Figure 11a. The model results aligned well with the field data, with absolute errors of 0.27 °C in July, 0.28 °C in August, and 0.22 °C in September. These values are within the commonly accepted error range of ±0.5 °C for thermal discharge studies [32], and are consistent with the pertinent literature [33]. This confirms that the model performs reliably under typical summer conditions. In addition, Figure 11b presents the validation results for two consecutive days in July 2021, corresponding to the buoy relocation. The comparison shows that the absolute errors are below 0.5 °C. The short-term validation with satisfactory accuracy demonstrates the model's ability to provide accurate results under varying observational conditions.

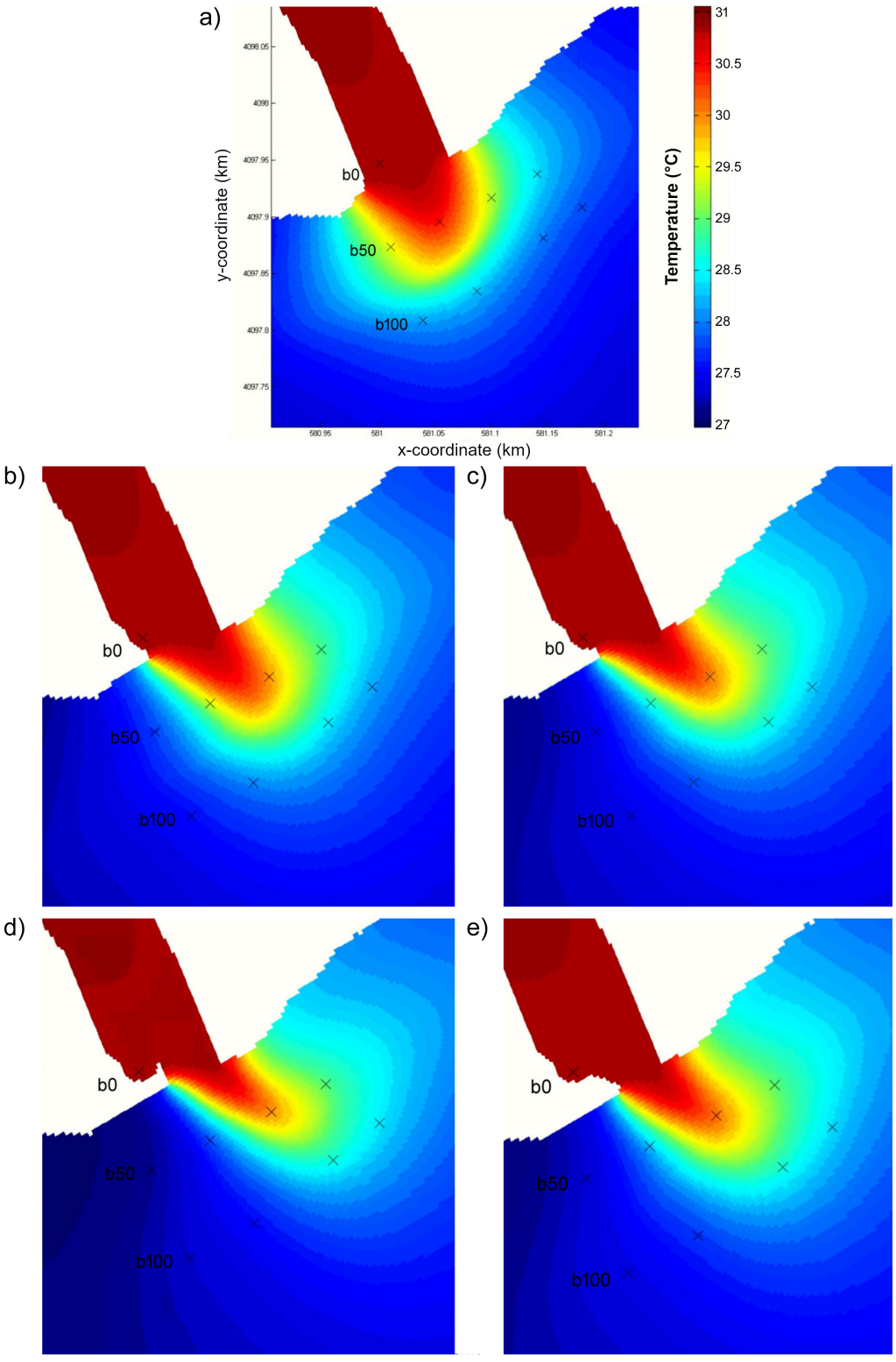

Figure 9. Temperature distribution during spit evolution at different lengths: (**a**) 0 m, (**b**) 10 m, (**c**) 20 m, (**d**) 30 m, and (**e**) 40 m. Cross marks indicate the repositioned measuring buoys.

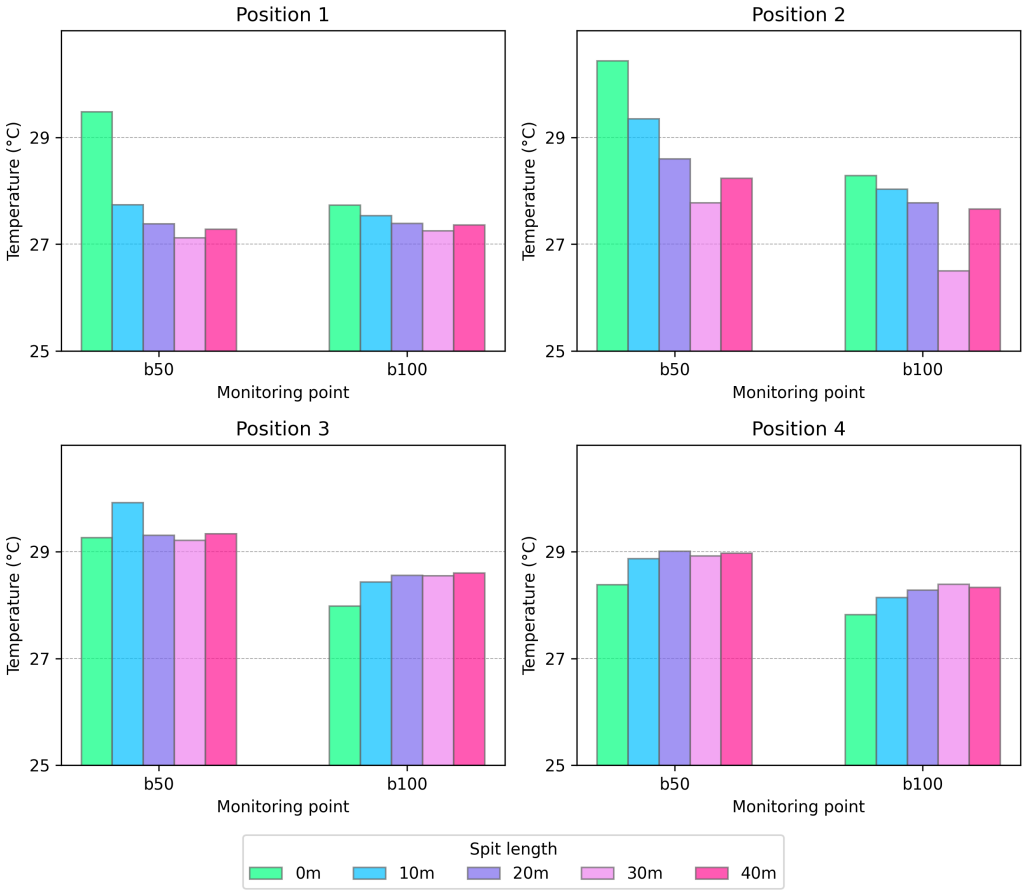

Figure 10. Temperature values at buoy locations under different spit length scenarios. Buoy positions are ordered from left to right in the study area.

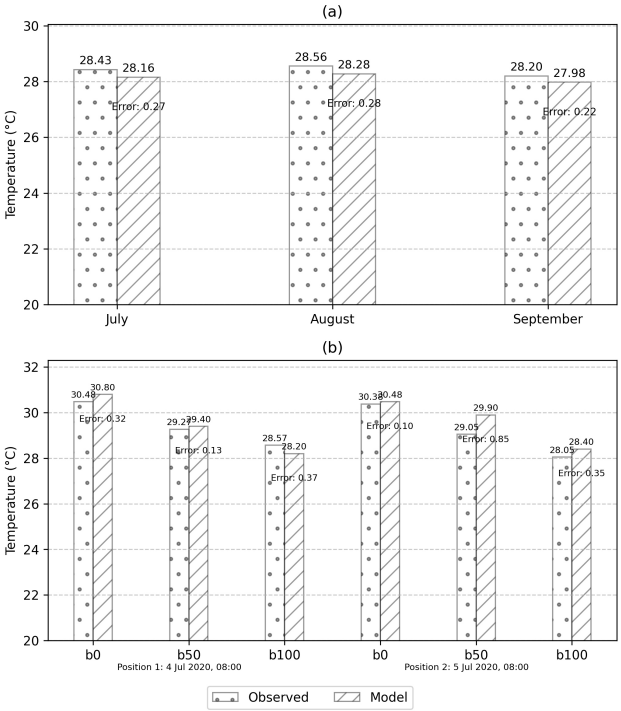

Figure 11. Comparison between observed and modeled water temperatures: (**a**) monthly mean temperatures and (**b**) daily temperatures over consecutive days.

4. Discussion

In this study, the impact of river mouth spit development on the dispersion of the thermal discharge in coastal environments was examined. The formation and evolution of spits influence the behavior of thermal plumes and characteristics of mixing zones by altering the local hydrodynamics. Thermal dispersion in dynamic coastal environments exhibits high instabilities, and initially symmetrical plumes become asymmetrical [34]. When the effluent of the cooling system is transported by a river into the sea, the river mouth morphology plays a crucial role in the dispersion characteristics. The spatiotemporal changes in river mouth spit cause uneven distribution of thermal plumes by altering the flow dynamics. Evolution of the spit from one side of the river mouth deflects the plume to the opposite side, modifying the direction and extension of mixing zone. This morphodynamic change can elevate the temperature in specific locations. As the warm plumes tend to spread laterally [35], the extension of temperature excess alongshore may exacerbate the near-field consequences.

The primary risk associated with poor mixing is the recirculation of the heated discharge back into the water intake [18]. This phenomenon can increase intake temperatures, reduce cooling efficiency, and potentially lead to operational damages [36]. Furthermore, the cumulative buildup of excess heat in the water body can degrade the aquatic environment [37]. In our study, however, the spit development shifts the thermal plume toward the west coast, while the intake is located far away from the river mouth on the east coast. Therefore, there is no risk of recirculating heated effluent into the intake system under the impact of river mouth morphodynamics.

One of the key findings of this study is that the removal of the spit significantly improves thermal mixing, thereby reducing the extent of temperature excess in the receiving water. Temperature measurements obtained from monitoring buoys under post-removal conditions indicate that thermal discharge increases ambient water temperature within a safe margin, remaining well below the international threshold of +3 °C at a distance of 100 m from the shoreline. Nevertheless, recent observations reveal an increase in temperature excess associated with the reformation of a new spit. These findings underline the need for management strategies that incorporate periodic dredging of the river mouth to maintain effective mixing zones and ensure continued compliance with environmental regulations.

5. Conclusions

The impact of river mouth spit development on the dispersion of thermal discharge from a coastal power plant was evaluated using a combination of field observations and numerical modeling. The study demonstrated that the thermal discharge successfully complies with the water pollution criteria defined in the regulations. Under both pre- and post-spit removal conditions, the temperature difference between thermal discharge and ambient water remained within acceptable limits in the edge of the mixing zone.

The oceanographic measurements provided consistent field data. Comparing the values during the study period and in recent years revealed that temperature excess strongly depends on the river mouth morphodynamics and meteorological conditions. The ambient water temperature associated with cold weather exhibited a greater difference compared to the temperature of the thermal discharge. In addition, numerical modeling indicated that ongoing spit evolution disrupts the symmetry of the thermal plume. As the spit extends, it deflects the plume toward the opposite shoreline, enlarging the mixing zone asymmetrically.

The findings demonstrated that spit removal enhanced dispersion efficiency and mitigated the temperature excess. On the contrary, the re-emergence of the spit triggered a rise in temperature differences in the area affected by the thermal discharge. Given the

dynamic nature of spit morphology, periodic dredging is recommended when spit growth significantly alters the direction of thermal dispersion. These results provide a quantitative basis for regulatory compliance strategies, demonstrating how monitoring and adaptive management of river mouth morphology can ensure adherence to environmental safety regulations (e.g., the +3 °C at 100 m thermal discharge limit) and support evidence-based environmental policy.

Author Contributions: Conceptualization: M.A., O.Y. and S.C.; formal analysis: N.H.; investigation: N.H., M.A., O.Y., M.Y.E., S.C. and M.V.; methodology: N.H. and M.A.; resources: N.H.; software: N.H.; validation: N.H. and O.Y.; data curation: M.A. and M.Y.E.; project administration: O.Y. and S.C.; supervision: M.A., O.Y., M.Y.E. and M.V.; writing—original draft: N.H.; visualization: N.H.; writing—review and editing: M.A., O.Y., M.Y.E., S.C. and M.V. All authors have read and agreed to the published version of the manuscript.

Funding: This research received no external funding.

Data Availability Statement: Data will be available from the first author upon request.

Acknowledgments: The authors acknowledge the support of HEC Engineering Ltd. and are appreciative for sharing the data used in this study.

Conflicts of Interest: The author Mehmet Yusuf Erbisim was employed by the company HEC Engineering Co., Istanbul, Türkiye. The remaining authors declare that the research was conducted in the absence of any commercial or financial relationships that could be construed as a potential conflict of interest.

References

1. Dodds, W.K.; Whiles, M.R. *Freshwater Ecology: Concepts and Environmental Applications of Limnology*, 2nd ed.; Elsevier: Amsterdam, The Netherlands, 2010. [CrossRef]
2. Micheletti, W.; Burns, J.M. Emerging issues and needs in power plant cooling systems. In *Proceedings of the Workshop "Electric Utilities and Water: Emerging Issues and R&D Needs"*; Electric Power Research Institute: Pittsburgh, PA, USA, 2002; pp. 1–5.
3. de Souza, J.N.M.; da C. Souza, A.R.; Melo, L.; Costa, A. The dynamic behavior of once-through cooling water systems under fouling phenomena. *Heat Transf. Eng.* **2021**, *43*, 1271–1279. [CrossRef]
4. Jovčevski, M.; Paunović, M.L.; Stojkovski, F.; Marko, M. Thermal pollution of a thermal power plant with once-through cooling systems: A numerical study. *Innov. Mech. Eng.* **2022**, *1*, 128–138.
5. Wang, H.; Qiu, B.; Zhao, F.; Yan, T.; Li, C. Research on enhancing power plant net power by integrating modeling heat transfer and operation optimization of once-through cooling water system. *Case Stud. Therm. Eng.* **2024**, *61*, 104966. [CrossRef]
6. Huang, Q.; Zhi, Y.; Zhang, R.; Du, X.; Zhang, J.; Wang, J. Flow heat transfer characteristics and dynamic response of once-through cooling water system in nuclear power plants under complex operating conditions. *Energies* **2025**, *18*, 1207. [CrossRef]
7. Gaeta, M.G.; Samaras, A.G.; Archetti, R. Numerical investigation of thermal discharge to coastal areas: A case study in South Italy. *Environ. Model. Softw.* **2020**, *124*, 104596. [CrossRef]
8. Bleninger, T.; Jirka, G.H. Mixing zone regulation for effluent discharges into EU waters. *Water Manag.* **2011**, *164*, 395–406. [CrossRef]
9. U.S. Environmental Protection Agency (EPA). *Water Quality Standards Handbook: Second Edition (Chapter 5: Mixing Zones)*; Technical Report; U.S. EPA, Office of Water: Washington, DC, USA, 1994.
10. Marmorino, G.; Savelyev, I.; Smith, G.B. Surface thermal structure in a shallow-water, vertical discharge from a coastal power plant. *Environ. Fluid Mech.* **2015**, *15*, 207–229. [CrossRef]
11. Kong, G.; Guan, W. Diffusion characteristics and mechanisms of thermal plumes from coastal power plants: A numerical simulation study. *J. Mar. Sci. Eng.* **2024**, *12*, 429. [CrossRef]
12. Braunschweig, F.; Chambel, P.; Martins, F.; Neves, R. A methodology to estimate the residence time of estuaries. *Ocean Dyn.* **2003**, *53*, 137–145. [CrossRef]
13. Salgueiro, D.V.; de Pablo, H.; Neves, R.; Mateus, M. Modelling the Thermal Effluent of a Near Coast Power Plant (Sines, Portugal). *Rev. Gestão Costeira Integr.* **2015**, *15*, 533–544. [CrossRef]
14. Thai, T.H.; Tri, D.Q. Modeling the Effect of Thermal Diffusion Process from Nuclear Power Plants in Vietnam. *Energy Power Eng.* **2017**, *9*, 403–418. [CrossRef]

15. Aljohani, N.S.; Kavil, Y.N.; Shanas, P.R.; Al-Farawati, R.K.; Shabbaj, I.I.; Aljohani, N.H.; Turki, A.J.; Abdel Salam, M. Environmental impacts of thermal and brine dispersion using hydrodynamic modelling for Yanbu desalination plant, on the eastern coast of the Red Sea. *Sustainability* **2022**, *14*, 4389. [CrossRef]
16. Durán-Colmenares, A.; Barrios-Piña, H.; Ramírez-León, H. Numerical modeling of water thermal plumes emitted by thermal power plants. *Water* **2016**, *8*, 482. [CrossRef]
17. Laguna-Zarate, L.; Barrios-Piña, H.; Ramírez-León, H.; García-Díaz, R.; Becerril-Piña, R. Analysis of thermal plume dispersion into the sea by remote sensing and numerical modeling. *J. Mar. Sci. Eng.* **2021**, *9*, 1437. [CrossRef]
18. Salehi, M. Thermal recirculation modeling for power plants in an estuarine environment. *J. Mar. Sci. Eng.* **2017**, *5*, 5. [CrossRef]
19. Petersen, D.; Deigaard, R.; Fredsøe, J. Modelling the morphology of sandy spits. *Coast. Eng.* **2008**, *55*, 671–684. [CrossRef]
20. Qi, Y.; Yu, Q.; Gao, S.; Li, Z.; Fang, X.; Guo, Y. Morphological evolution of river mouth spits: Wave effects and self-organization patterns. *Estuar. Coast. Shelf Sci.* **2021**, *262*, 107567. [CrossRef]
21. Anthony, E.J. Wave influence in the construction, shaping and destruction of river deltas: A review. *Mar. Geol.* **2015**, *361*, 53–78. [CrossRef]
22. Cheng, Y.L.; Hao, Q.Z.H.J. Effects of topography on diffusion of thermal discharge in power plant. *Procedia Environ. Sci.* **2011**, *11*, 618–623. [CrossRef]
23. Dan, S.; Walstra, D.J.R.; Stive, M.J.F.; Panin, N. Processes controlling the development of a river mouth spit. *Mar. Geol.* **2011**, *280*, 116–129. [CrossRef]
24. Saengsupavanich, C. Morphological evolution of sand spits in Thailand. *Mar. Geod.* **2021**, *44*, 432–453. [CrossRef]
25. Taveneau, A.; Almar, R.; Bergsma, E.W. On the cyclic behavior of wave-driven sandspits with implications for coastal zone management. *Estuar. Coast. Shelf Sci.* **2024**, *303*, 108798. [CrossRef]
26. Kouwen, N.C.; Ton, A.M.; Vos, S.E.; Vijverberg, T.; Reniers, A.J.H.M.; Aarninkhof, S.G.J. Quantifying spit growth and its hydrodynamic drivers in wind-dominated lake environments. *Geomorphology* **2023**, *437*, 1–18. [CrossRef]
27. Pradhan, U.; Mishra, P.; Mohanty, P.K.; Behera, B. Formation, growth and variability of sand spit at Rushikulya River mouth, South Odisha Coast, India. *Procedia Eng.* **2015**, *116*, 963–970. [CrossRef]
28. Zhang, S.; Tian, C.; Zhou, F. Ocean Observation System Design of Mooring Buoy and Benthic Node with Electro-Optical-Mechanical Cable. *Front. Mar. Sci.* **2022**, *9*, 1018751. [CrossRef]
29. Leeder, M.R.; Bridges, P.H. Flow separation in meander bends. *Nature* **1975**, *253*, 338–339. [CrossRef]
30. Heidari, N.; Yagci, O.; Aksel, M. Midchannel islands in lowland river corridors and their impacts on flow structure and morphology: A numerical based conceptual analysis. *Ecol. Eng.* **2022**, *173*, 106419. [CrossRef]
31. Heidari, N.; Aksel, M.; Yağci, O.; Valyrakis, M. A numerical study of the flow patterns around midchannel islands in lowland rivers and their possible biogeomorphological impacts. *Int. J. Environ. Geoinformatics* **2023**, *10*, 154–175. [CrossRef]
32. United States Environmental Protection Agency (USEPA). *Technical Guidance Manual for Performing Waste Load Allocations*; Technical Report; USEPA: Washington, DC, USA, 2001.
33. Prats, J.; Val, R.; Dolz, J.; Armengol, J. Water temperature modeling in the Lower Ebro River (Spain): Heat fluxes, equilibrium temperature, and magnitude of alteration caused by reservoirs and thermal effluent. *Water Resour. Res.* **2012**, *48*, W05523. [CrossRef]
34. Marques, F.; Lopez, J.M. Impact of nonuniform ambient stratification on thermal plume dynamics. *Phys. Fluids* **2013**, *25*, 043602. [CrossRef]
35. Moulton, M.; Chickadel, C.C.; Thomson, J. Warm and cool nearshore plumes connecting the surf zone to the inner shelf. *Geophys. Res. Lett.* **2021**, *48*, e2020GL091675. [CrossRef]
36. Hao, R.; Qiao, L.; Han, L.; Tian, C. Experimental study on the effect of heat-retaining and diversion facilities on thermal discharge from a power plant. *Water* **2020**, *12*, 2267. [CrossRef]
37. Langford, T.E. *Ecological Effects of Thermal Discharges*; Springer: Berlin/Heidelberg, Germany, 1990. [CrossRef]